VOL. 18, NO. 7, APRIL 2023 ISSN 1819-6608
ARPN Journal of Engineering and Applied Sciences

www.arpnjournals.com

EFFECT OF OIL PALM BOILER ASH MODIFIED WITH PEG 6000 ON MECHANICAL PROPERTIES OF HIGH-DENSITY POLYETHYLENE

Karya Sinulingga[1], Nurdin Bukit[1], Abd Hakim S.[1] and Bunga Fisikanta Bukit[2]
[1]Department of Physics, Universitas Negeri Medan, Medan, Indonesia
[2]Department of Physics, Universitas Quality Berastagi, Berastagi, Indonesia
E-Mail: nurdinbukit5@gmail.com

ABSTRACT

The mechanical properties of material play an essential role in the material. Mechanical properties are one of the properties possessed by a material to function for various applications. Using nanostructured materials such as silica and layered silicates as fillers can significantly change the properties of the polymer matrix. OPBA preparation was carried out using calcination and ball mill methods, coprecipitation, and the addition of PEG 6000. Various methods were carried out to obtain OPBA with optimal silica content. HDPE thermoplastic was prepared with OPBA filler by mixing HDPE thermoplastic with OPBA nanoparticles modified with PEG 6000. SEM OPBA calcination and ball mill show the presence of pores on the surface. Meanwhile, the pore in OPBA does not lead to coprecipitation. However, in OPBA with added PEG 6000, it was seen again that there were pores on the surface and the presence of agglomerate dispersions in OPBA preparation with PEG 6000 showed the addition of functional groups to OPBA. The dispersion peaks of the silica contained in OPBA with state characteristics at 20^o–30^o appear in the XRD patterns of unmodified silica and modified silica, indicating that the precipitated silica is amorphous silica and the surface modification does not change the phase structure of the modified silica. In addition, the optimal silica content is found in OPBA PEG 6000, with a silica content of 60.7%. The addition of OPBA PEG 6000 filler generally increases the mechanical properties of tensile strength, elongation at break, and elongation modulus.

Keywords: silica, waste, polymer, thermoplastic, filler.

Manuscript Received 21 December 2022; Revised 8 May 2023; Published 30 May 2023

1. INTRODUCTION

Using nanostructured materials such as silica and layered silicates as fillers can profoundly change the polymer matrix's properties. Adding small amounts of nanofiller (usually less than 10% by weight) to polymers can improve their mechanical properties [1]. Research on silica synthesized from waste ash as filler in polymers has yet to be widely found. Silica from waste ash consists of various nanoparticles in multiple sizes (specific areas ranging from 50 to 400 m2 g−1) and with different surface treatments from hydrophilic to hydrophobic. Due to their fractal structure and the high specific area, fumed silicas are subject to self-aggregation and consequently can form networks of connected or interacting particles in polymers [2], [3].

Oil palm boiler ash (OPBA) is a siliceous waste that can be used as a filler and provides economical and environmentally friendly benefits. OPBA is ash that has undergone a process of burning fruit shells and fibers at a temperature of 500°C - 700°C in a boiler furnace. Palm ash is the residue from burning the shells and threads of the oil palm fruit [4]–[6]. Boiler ash has a chemical composition that resembles other aluminosilicates, such as clay. This material solidifies while in the exhaust gases and is collected using an electrostatic precipitator. Because these particles condense while suspended in the exhaust gases, the ash particles are generally spherical ash particles that collect on the electrostatic precipitator. Many methods have been explored to synthesize SiO_2 raw materials, as they are suitable for a wide range of applications and cost-effective simultaneously. The extraction and methodology of synthesis of silica from agricultural wastes and other derivatives mainly aim to produce high-purity silica with low contaminants at an affordable cost with higher prospects for large-scale production. Innovative research studies have reported incorporating waste-derived silica nanoparticles with several polymers. The environmental aspect of the synthesis process is also considered by improving conventional methods and replacing specific steps and chemicals with environmentally friendly ones. Synthesis of silica from agricultural waste is carried out by several methods, such as sol-gel, combined acid leaching, chemical dissolution, co-assembly with added surfactants, calcination, mechanical milling, and coprecipitation [7], [8].

The sol-gel process successfully produced Submicron silica particles and was used to create HDPE/SiO_2 composites. The addition of silica submicron particles to HDPE causes an increase in its mechanical properties. High-density polyethylene (HDPE) is a type of thermoplastic polymer that is attracting attention to be developed, one of which is. HDPE as a matrix has advantages over other types of thermoplastics due to its unique properties, which include tensile strength [9]. In addition, HDPE is a type of polymer with high density that is flexible, resistant to impact, and low-temperature resistance. HDPE is a thermoplastic commodity that is 100% recyclable and can function well as a composite matrix because it has Young's modulus and high tensile

strength. HDPE is usually dark and opaque and can appear in a variety of colors, although it is usually white.

The properties of a filler to be compatible with the polymer matrix are influenced by several factors, among others, the particle size of the filler, where the small particle size of the filler can increase the degree of strengthening of the polymer compared to a larger size. Likewise, the smaller the particle size, the higher the bond between the filler and the polymer matrix. OPBA preparation into nanoparticles can be carried out by various methods such as calcination, ball mill, coprecipitation, and the addition of surfactants. The addition of surfactants such as PEG-6000 is done because it has stable properties, mixes easily with other components, and is not irritating [6], [10]–[13]

2. MATERIALS AND METHODS

2.1. Material

This research was carried out in the laboratory of Universitas Negeri Medan. The materials used are Oil Palm Boiler Ash from palm oil mill 5M HCl, NH_4OH Merck Pro Analis, PEG 6000 Merck, and Aquades.

2.2. Methods

a. Preparation of OPBA Nanoparticle by calcination and ball mill methods, coprecipitation and modification of PEG 6000

Obtained from palm oil processing was calcined at a temperature of 500°C for 5 hours and milled for 10 hours with a rotation of 250 rpm. Furthermore, OPBA was mixed with 5 M HCl in a ratio of 1:4, stirred, and heated with a magnetic stirrer at 70°C for 4 hours at a speed of 400 rpm. The OPBA, mixed with 5M HCL, was filtered using filter paper, then mixed again with NH4OH in a ratio of 1:4, stirred, and heated with a Magnetic Stirrer at 70°C for 4 hours at a speed of 400 rpm. The OPBA synthesis was continued by mixing PEG 6000. PEG 6000 was melted first using a magnetic stirrer at 70°C for 60 minutes. The OPBA was then mixed with melted PEG 6000 and distilled water in a ratio (1:3:6) using a magnetic stirrer at 70°C for 4 hours at a speed of 400 rpm. The solution was filtered and dried at 100°C for 4 hours. The resulting OPBA was further characterized by Scanning Electron Microscope (SEM), Fourier-transform infrared spectroscopy (FTIR), and X-ray diffraction (XRD).

b. Preparation of HDPE Thermoplastic with OPBA PEG 6000 Filler

The preparation of HDPE thermoplastic with OPBA filler was carried out by mixing HDPE thermoplastic with OPBA nanoparticles modified with PEG 6000. Mixing was carried out with the Rheomixer HAAKE Polylab OS System at a rate of 60 rpm for 10 minutes at 150°C. From the internal mixer process (in granular form). Injection molding is carried out with ASTM 638 type V with a molding temperature of 150°C, with a strength of 750 bar. The composition of the mixed ingredients in the Rheomixer HAAKE Polylab OS is shown in Table-1.

Table-1. The composition of the mixed ingredients in the Rheomixer HAAKE Polylab OS.

Material	S_0	S_1	S_2	S_3	S_4
HDPE (%wt)	100	98	96	94	92
OPBA modified with PEG 6000 (%wt)	0	2	4	6	8

3. RESULT AND DISCUSSIONS

3.1 Fourier-Transform Infrared Spectroscopy (FTIR) Characterization

The FTIR used is the Agilent Cary 630 FTIR. This flexible benchtop FTIR instrument that offers high performance and exceptional ease of use in an ultra-compact design. Each signal is caused by energy absorbed at a certain frequency from infrared radiation, resulting in bond vibrations within the molecule. Multiple signals are very easy to use to identify a particular type of bond in a molecule. Each signal is caused by energy absorbed at a specific frequency from infrared radiation, causing bond vibrations in the molecule. Some signals are straightforward to use to identify specific types of bonds in molecules. The region to the right of the diagram (1500 to 500 cm-1) usually contains very complex absorbent forms.

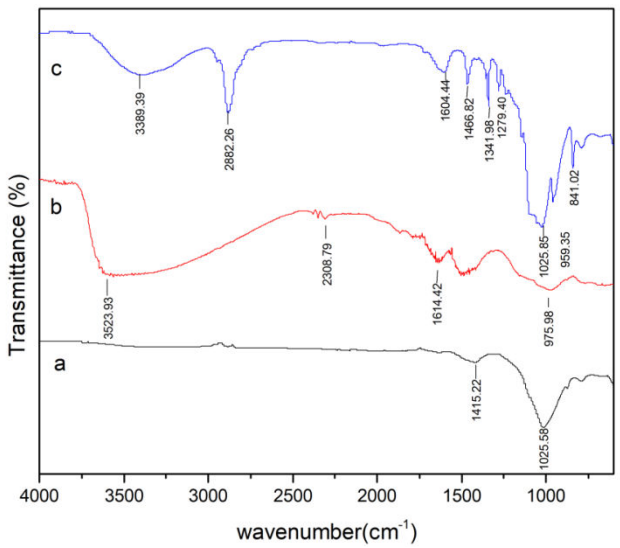

Figure-1. FTIR graph of: a). OPBA calcination and ball mill, b). OPBA coprecipitation, c). modification OPBA with added PEG 6000.

Figure-1 shows the absorption peaks in OPBA calcination and ball mill, coprecipitation, and modification of PEG 6000. From Table-2 it can be seen that there is an addition of functional groups from coprecipitation OPBA and OPBA with added PEG 6000. However, in general, all samples show the presence of Si-O-Si stretching modes and bending vibration of Si-O. The addition of PEG 6000 causes the OH absorption band to look sharper compared

to other samples. This process on silica nanoparticles causes the presence of more OH groups. It is crucial because the quantification of silanol groups and the amount of silanol is essential in evaluating silica nanoparticle chemical reactivity. The surface area of chemical modifications of silica, such as branching with organic functional groups and insertion of metal ions, is highly dependent on the concentration of silanol groups in each silica [14], [15].

Table-2. The functional groups of OPBA.

Wavenumber (cm^{-1}) OPBA Calcination and Ballmill	Functional Group	Wavenumber (cm^{-1}) OPBA Coprecipitation	Functional Group	Wavenumber (cm^{-1}) OPBA with added PEG 6000	Functional Group
1025.58	Symmetric and symmetric stretching mode at SiO-Si	975.98	Bending vibration of Si-O	841.02	Bending vibration of Si-O
1415.22	Si-O-Si stretching modes	1614.42	Bending vibration of O-H	959.35	Bending vibration of Si-O
-	-	2308.79	Bending vibration of O-H	1025.85	Symmetric and symmetric stretching mode at SiO-Si
-	-	3523.93	Bending vibration of O-H	1279.40	Si-O-Si stretching modes
-	-	-	-	1341.98	Si-O-Si stretching modes
-	-	-	-	1466.82	H_2O adsorbed between silicate layers
-	-	-	-	1604.44	Bending vibration of O-H
-	-	-	-	2882.26	Bending vibration of O-H
-	-	-	-	3389.39	Bending vibration of O-H

3.2 Scanning Electron Microscope (SEM) Characterization

SEM characterization was carried out using the SEM TM 3030 model Hitachi High-Tech has provided a 5kV mode that allows for sharper observations of the surface structure of the finest samples, which cannot be observed at high accelerating voltages. Figure-2 shows the Morphology of OPBA. In general, boiler ash is the remaining solid waste resulting from biomass combustion, which is heterogeneous with the main components of silica, alumina, iron oxide, and calcium oxide with various amounts of carbon, depending on the mineralogical composition of the burned biomass and the method of combustion [16].

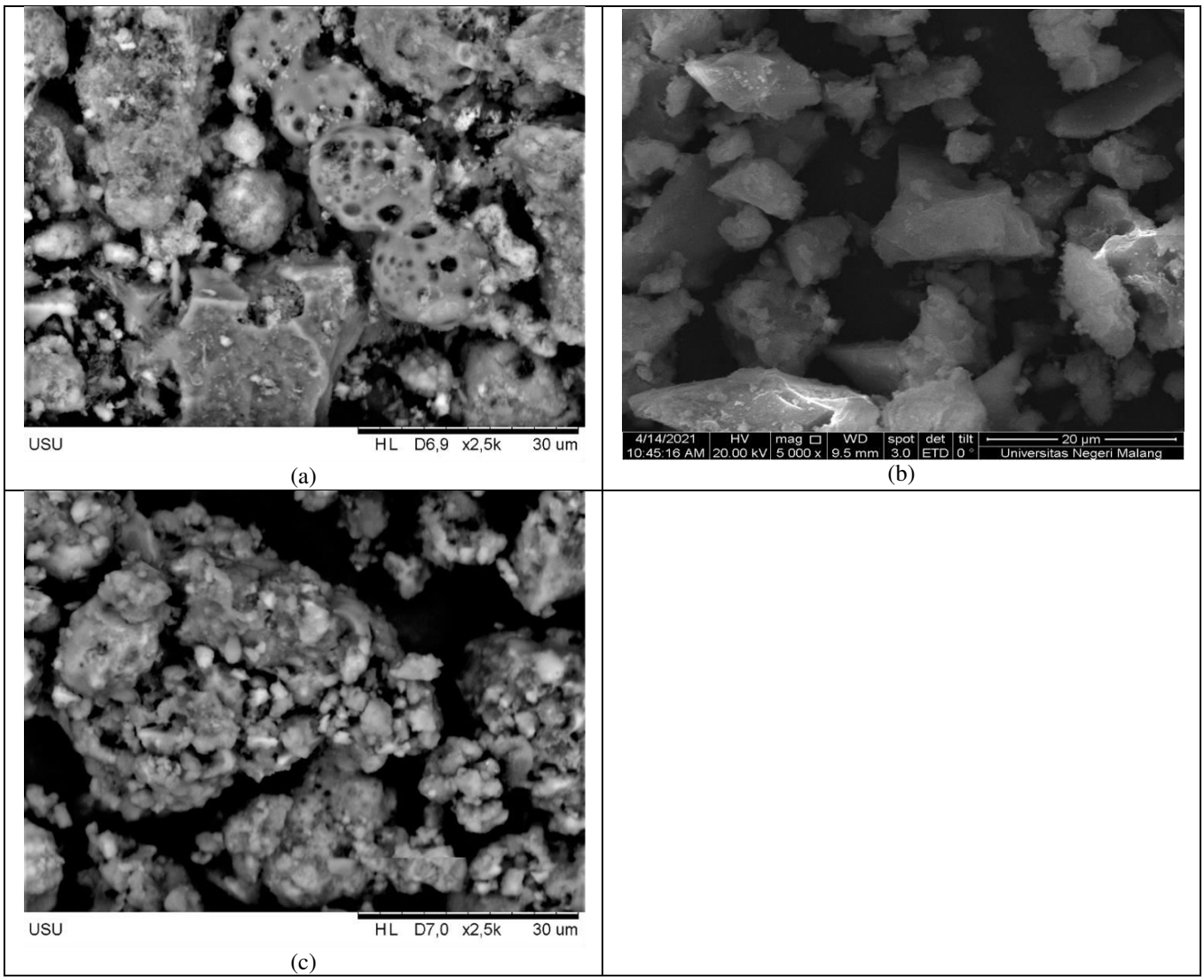

Figure-2. Morphology of: a). OPBA calcination and ball mill, b). OPBA coprecipitation, c). modification OPBA with added PEG 6000.

Figure-2 SEM OPBA calcination and ball mill show the presence of pores on the surface. Meanwhile, the pore in OPBA does not lead to coprecipitation. After acid treatment with HCL in the coprecipitation process, some parts of the OPBA were split into several parts, and the outer surface of the epidermis was peeled off. Several tiny pores remain in the inner epidermis of OPBA. A relatively smooth, flat plate-like layer with a few lumps on top. This is due to the influence of NaOH, which makes the flat plate layer smoother. Previous studies on the hydration process of siliceous materials such as coal fly ash with calcium hydroxide and calcium sulfate produced complex ions Ca, Al, and O. These complex ions were also observed in the synthesized OPBA samples [17]. However, in OPBA with added PEG 6000, it was seen again that there were pores on the surface and the presence of agglomerate dispersions. The irregular morphology of silica is associated with the presence of silica agglomeration. The silica particles become smaller and more agglomerated when the calcination temperature increases. It is mainly due to minerals in crystalline form at higher temperatures becoming more brittle. In addition, it can be observed that the ash produced after calcination is not too bound with other impurities. Impurities are assumed to be reduced in the calcination process. In general, silica is irregular and is grouped into spherical shapes. Irregular shapes, assumed silica, can be detected in all SEM images [18].

3.3 X-Ray Diffraction (XRD) Characterization

XRD characterization is useful for obtaining diffraction patterns and crystal structures. The XRD used is the Shimadzu 6100 type (40 kV, 30 mA) with a wavelength of Cu-Kα1 =1.5405 = 0.15406 nm, with a rate of 2°/min at an angle range of 2Θ = 10 °- 70°. Figure-3 shows the XRD data of OPBA. By using the Match-Phase Identification from Powder Diffraction Data application, using the COD database (Crystallography Open Database) it is possible to identify compounds that match the peaks at an angle of 2θ given from the analysis results.

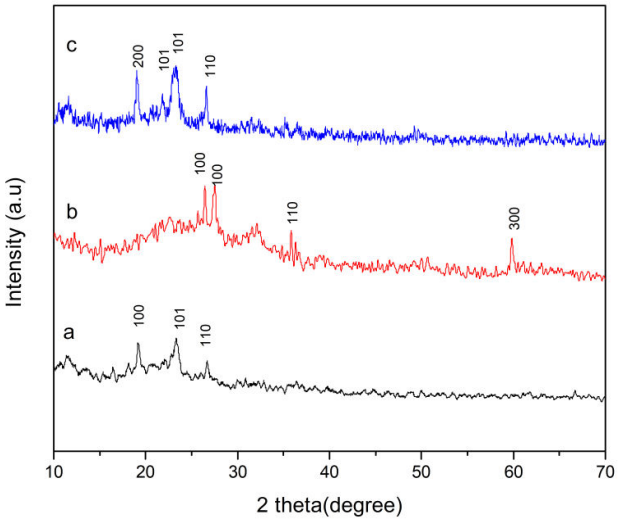

Figure-3. XRD pattern of: a). OPBA calcination and ball mill, b). OPBA coprecipitation, c). Modification OPBA with added PEG 600.

Figure-3 shows the dispersion peaks of the silica contained in OPBA with state characteristics at 20^{o}-30^{o} appear in the XRD patterns of unmodified silica and modified silica, indicating that the precipitated silica is amorphous silica and the surface modification does not change the phase structure of the modified silica. [19]. According to the surface chemistry model of amorphous silica, the surface of silica consists of free water, single silanol, germinal-silanol groups, vicinal-silanols, and siloxane. Moreover, the modified silica also comes from the organic group. Under various conditions, amorphous silica is considered more reactive than crystalline silica [20]. The reactivity of amorphous silica is caused by the presence of hydroxyl groups (silanol) obtained after heating to a temperature of 400°C. This silanol group (-SiOH) can be found on the silica sample's surface, which causes a reactive region formation [21]–[24]. The reaction after the treatment after the coprecipitation process with a highly alkaline solution of HCL and NaOH causes the silica in the ash to react with NaOH to form a new molecular structure of sodium silicate (Na_2SiO_3) and water as a residue. At the same time, HCL reacts and removes all inorganic compounds, such as carbonates. Thus forming amorphous silica nanoparticles [25].

Table-3. XRD Data of OPBA.

XRD Data	OPBA calcination and Ballmill	OPBA coprecipitation	Modification OPBA with added PEG 6000
Crystal system	Orthorombic	Orthorombic	Trigonal
Space Group	P 21 212 (18)	P mma (51)	P 32 2 1 S (-1)
The lattice meter	A= 11,60000A	A= 25,11060A	A= 4,92090 A
	c= 5,20000 A	c= 12,85960 A	c= 5,40910 A
Density	2,281 g/cm^3	1,82900 g/cm^3	2,639 g/cm^3
2 thetaangle	19,32	27,31	23,32
Maximumd_{hkl} Intensity 1	101	010	101
Latticedistanced d (Å)	4,7450	12,4972	3,3475
2 thetaangle	23,46	26,21	19,08
Maximumd_{hkl} Intensity 2	210	210	100
Latticedistanced d (Å)	5,1877	8,8573	4,2616
2 thetaangle	26,80	35,59	26,62
Maximumd_{hkl} Intensity 3	311	200	112
Latticedistanced d (Å)	2,9975	12,5553	1,8200

3.4 X-Ray Fluorescence (XRF) Characterization

The principle used is the determination of the elemental composition based on X-ray interactions with matter. The advantage of the XRF method is its high accuracy high, can determine the elements in the material in the absence of standards, and can determine the mineral content in biological materials directly. The characteristic X-ray intensity for each element under investigation is determined by rotating the crystal and detector at the required angle to diffract the length characteristic wave. The X-ray intensity was then measured for each element and each element at a known concentration standard. The XRF tool used in this study is the PANalytical type Minipal 4. XRF characterization is shown in Table-4.

Table-4. Compound of OPBA from XRF characterization.

Compound	OPBA calcination and ball mill (%)	OPBA coprecipitation (%)	Modification OPBA with added PEG 6000 (%)
SiO_2	48.4	48.1	60.7
K_2O	8.73	11.8	3.67
CaO	29.7	21.1	19.8
Fe_2O_3	4.22	11.4	6.37
TiO_2	0.46	1	0.60
MnO	0.29	0.53	0.40
Cr_2O_3	0.047	0.38	0.11
ZnO	0.061	-	0.65
CuO	0.15	0.12	0.23
NiO	-	-	0.03
V_2O_5	0.01	0.007	0.010
P_2O_5	6.86	-	7.26
SrO	0.10	0.22	-
BaO	0.02	0.24	-
Eu_2O_3	0.09	0.2	0.1
Re_2O_7	0.09	0.2	0.1
Rb2O	-	0.36	-
MgO	-	4	-

In general, OPBA has dominant silica content, followed by Cao and K_2O. There was an increase in SiO_2. In OPBA coprecipitation, the amount of SiO_2 has increased. It is caused by the reaction of HCl with OPBA in the coprecipitation process. Coprecipitation is a bottom-up synthesis method used to obtain nanometer-sized small particles. This method has the principle of removing the continuous bond that is owned by a metal compound in liquid form without considering the specific mechanism that occurs. The versatility and simplicity of the coprecipitation method make it one of the better techniques for preparing nanoparticles. The addition of HCL causes the anion of the silicate to turn into silanol so that when the silanol reacts with the anion, the silicate returns to form siloxane. In addition, the HCL solution also has protons from hydrochloric acid, which are capable of forming silicic acid in the precipitation process [26]. Furthermore, the highest SiO_2 content was found in OPBA with added PEG 6000. This increase is likely to have occurred in the quantitative test analysis. Suppose the level of a compound in the sample decreases. In that case, it may be accompanied by an increase in other compounds because the amount of compound content is determined by comparing all the compounds in the sample.PEG 6000 is used to shape and control pore size and structure. 6000 states the molecular weight with increasing the molecular weight of PEG can increase its solubility in water. In addition, PEG 6000 is a polymer consisting of several monomer bonds. The monomer is a compound that can be polymerized. PEG 6000 has stable properties, dissolves easily in warm water, is non-toxic, non-corrosive, odorless, colorless, has a very high melting point (580°F), spreads evenly, evaporates efficiently, and can also bind pigments[13], [27]-[30].

SiO_2 and CaO are easily retained because they are non-volatile. In addition, there was an increase in SiO_2. This increase is likely to occur in the analysis of quantitative tests. Suppose the level of a compound in the sample decreases. In that case, it may be accompanied by an increase in other compounds because the amount of compound content is determined by comparing all the compounds in the sample. The principal weight loss of ABKS is decomposition and volatilization (evaporation). A comparison of the ash obtained at different temperatures found that 500 °C is the most appropriate for analyzing boiler ash in industrial applications.

3.5 Mechanical Properties

The mechanical properties of HDPE thermoplastics with filler-modified OPBA PEG 6000 were tested using the Universal Testing Machine (UTM) Shimadzu AGS-X series 10 kN. Mechanical properties such as hardness, elongation at break, tensile strength, and Young's modulus, of the compound were analyzed as a function of the weight percentage of filler shown in Figure-4. In tensile testing, the essential mechanical

properties of a molded material or specimen taken from a specified area of a component are determined. The characteristic values are the tensile stress which is the force applied to the initial cross-section of the specimen. Next is the tensile modulus, which is the gradient of the curve in the stress-strain diagram. The yield point is the stress and strain at the point of the curve plot where the gradient is zero. The breaking point is the stress and strain when the specimen breaks. The Poisson's ratio is the negative ratio of transverse strain to axial strain. Tensile tests up to ASTM D638 yield critical mechanical properties, including tensile stress, strain, tensile modulus, yield point, breakpoint, and Poisson's ratio. The conditioning and ambient conditions specified in ASTM D638 for the specified conditions and ambient conditions for temperature and humidity are of paramount importance for the comparison of test results. Specifications for the duration of conditioning can usually be found in the material standard for the plastic being tested. Furthermore, specimens used in tests on impression materials shall be stored in a standard atmosphere (standard temperature and humidity conditions) for at least 16 hours before the test.

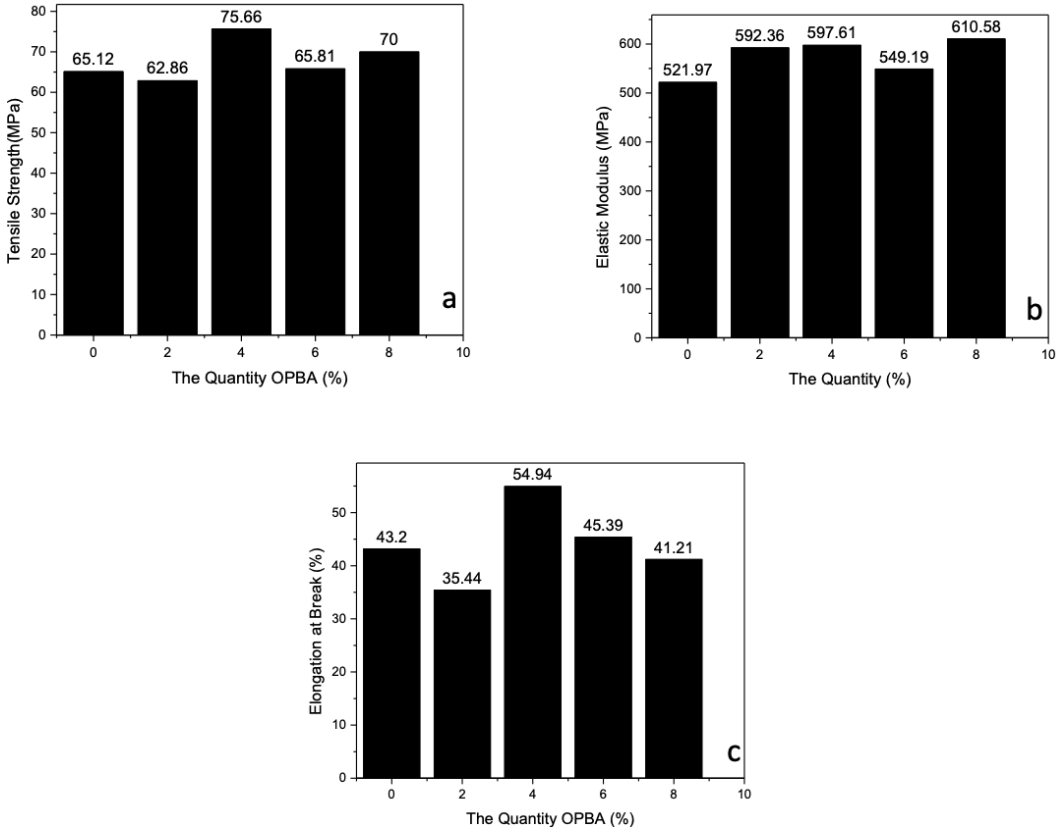

Figure-4. Mechanical properties: a). Tensile strength, b). Elongation at break, c). Elongation Modulus of HDPE thermoplastics with filler-modified OPBA PEG 6000.

Table-5. Mechanical properties of HDPE thermoplastics with filler-modified OPBA PEG 6000.

Sample	Tensile strength (MPa)	Elongation at Break (%)	Elongation Modulus (MPa)	Maximum point load (N)
S_0	65.12	43.20	521.97	586.13
S_1	62.86	35.44	592.36	565.77
S_2	75.66	54.94	597.61	680.99
S_3	65.81	45.39	549.19	592.29
S_4	70.00	41.21	610.58	630.08

Mechanical analysis is carried out to determine the mechanical properties of a material, including analysis of tensile strength, yield strength, elongation at break, elastic modulus, and other tests. Mechanical properties depend on an extensive range of higher molecular weights. Mechanical properties are usually studied by observing the tensile strength properties using tensometers and dynamometers. During this time, the specimen is deformed under the influence of tension. Based on the mechanical test results on HDPE with OPBA PEG 6000

filler, tensile strength, elongation at break, and maximum point load showed an increase in the overall HDPE filled with OPBA PEG 6000 filler. This increase in mechanical properties is due to the excellent interaction between polymer and filler. OPBA is responsible for the proper dispersion in the rubber matrix. As a result, load transfer between the matrix and filler increases, as well as the stiffness of the soft rubber matrix. In summary, the improvement in physical properties implies direct evidence for an increase in the contact surface area between the filler and the matrix [31]. Effective dispersion and absence of aggregate formation have resulted in the formation of a stronger bond between the matrix and filler, which results in increased tensile power to the matrix [32].

4. CONCLUSIONS

SEM OPBA calcination and ball mill show the presence of pores on the surface. Meanwhile, the pore in OPBA does not lead to coprecipitation. However, in OPBA with added PEG 6000, it was seen again that there were pores on the surface and the presence of agglomerate dispersionsOPBA preparation with PEG 6000 showed the addition of functional groups to OPBA. The dispersion peaks of the silica contained in OPBA with state characteristics at 20^{o}–30^{o} appear in the XRD patterns of unmodified silica and modified silica, indicating that the precipitated silica is amorphous silica and the surface modification does not change the phase structure of the modified silica. In addition, the optimal silica content is found in OPBA PEG 6000, with a silica content of 60.7%. The addition of OPBA PEG 6000 filler generally increases the mechanical properties of tensile strength, elongation at break, and elongation modulus. This increase in mechanical properties is due to the excellent interaction between polymer and filler. OPBA is responsible for the proper dispersion in the rubber matrix.

ACKNOWLEDGMENTS

This research was funded by the DIPA Fund of the Directorate of Research, Technology and Community Service, Directorate General of Higher Education, Research and Technology. Ministry of Education, Research Culture, and Technology for Fiscal Year 2022 according to No SP DIPA 023.17.1.690523/2022 02th revision dated 22 April 2022 and Number 022/UN33.8/DRTPM/PL/2022.

REFERENCES

[1] A. Dorigato, M. D'Amato and A. Pegoretti. 2012. Thermo-mechanical properties of high-density polyethylene - Fumed silica nanocomposites: Effect of filler surface area and treatment. Journal of Polymer Research, 19(6), doi: 10.1007/s10965-012-9889-2.

[2] W. H. Kwan and Y. S. Wong. 2020. Acid leached rice husk ash (ARHA) in concrete: A review. Mater Sci Energy Technol, 3: 501-507, doi: 10.1016/j.mset.2020.05.001.

[3] R. D. Devi and A. Ganapathi. 2022. Se-doped SiO2 nancomposite material synthesis, characterization and multi applications. Mater Sci Energy Technol, 5: 161-170, doi: 10.1016/j.mset.2022.01.004.

[4] N. Bukit, E. M. Ginting, E. Frida and B. F. Bukit. 2022. Preparation of Environmentally Friendly Adsorbent Using Oil Palm Boiler Ash, Bentonite and Titanium Dioxide Nanocomposite Materials. 23(12): 75-82.

[5] B. F. Bukit, E. Frida, S. Humaidi, P. Sinuhaji and N. Bukit. 2022. Optimization of Palm Oil Boiler Ash Biomass Waste as a Source of Silica with Various Preparation Methods. 23(8): 193-199.

[6] E. M. Ginting, N. Bukit, E. Frida and B. F. Bukit. 2020. Microstructure and thermal properties of natural rubber compound with palm oil boilers ash for nanoparticle filler. Case Studies in Thermal Engineering, doi: 10.1016/j.csite.2019.100575.

[7] N. S. Osman and N. Sapawe. 2020. Optimization of silica (SiO2) synthesis from acid leached oil palm frond ash (OPFA) through sol-gel method. Mater Today Proc, 31(xxxx): 232-236, doi: 10.1016/j.matpr.2020.05.300.

[8] M. R. M. Asyraf *et al*. 2022. Mechanical properties of oil palm fibre-reinforced polymer composites: a review. Journal of Materials Research and Technology, 17: 33-65, doi: 10.1016/j.jmrt.2021.12.122.

[9] O. O. Daramola, I. O. Oladele, B. O. Adewuyi, R. Sadiku and S. C. Agwuncha. 2015. Influence of Submicron Agro Waste Silica Particles and Vinyl Acetate on Mechanical, Diffusivity and Thermal Properties of High Density Polyethylene Matrix Composites Department of Metallurgical and Materials Engineering, Federal University of Technology. (June): 382.

[10] E. Frida, N. Bukit, F. R. A. Bukit and B. F. Bukit. 2022. Preparation and characterization of Bentonite-OPBA nanocomposite as filler. J Phys Conf Ser, 2165(1), doi: 10.1088/1742-6596/2165/1/012023.

[11] E. Frida, F. Rahmat, A. Bukit and F. Bukit. 2022. Analysis Structure and Morphology of Bentonite-Opba. 20: 117-125.

[12] E. M. Ginting, N. Bukit, E. Frida and B. F. Bukit. 2020. Microstructure and thermal properties of natural rubber compound with palm oil boilers ash for nanoparticle filler. Case Studies in Thermal Engineering, 17(November 2019): 100575, doi: 10.1016/j.csite.2019.100575.

[13] N. Bukit, E. M. Ginting, I. S. Pardede, E. Frida and B. F. Bukit. 2018. Mechanical properties of composite thermoplastic hdpe / natural rubber and palm oil boiler ash as filler. J Phys Conf Ser, 1120(1), doi: 10.1088/1742-6596/1120/1/012003.

[14] W. Zhuang *et al.* 2017. Facile synthesis of amino-functionalized mesoporous TiO2 microparticles for adenosine deaminase immobilization. Microporous and Mesoporous Materials, 239: 158-166, doi: 10.1016/j.micromeso.2016.09.006.

[15] P. Gogoi, D. Dutta and T. K. Maji. 2017. Equilibrium and kinetics study on removal of arsenate ions from aqueous solution by CTAB/TiO2 and starch/CTAB/TiO2 nanoparticles: A comparative study. J Water Health, 15(1): 58-71, doi: 10.2166/wh.2016.127.

[16] B. F. Bukit, E. Frida, S. Humaidi and P. Sinuhaji. 2022. Selfcleaning and antibacterial activities of textiles using nanocomposite oil palm boiler ash (OPBA), TiO2 and chitosan as coating. S Afr J Chem Eng, 41(February): 105-110, doi: 10.1016/j.sajce.2022.05.007.

[17] S. Y. Lau, S. L. Phuan, M. K. Danquah and C. Acquah. 2019. Sustainable palm oil refining using pelletized and surface-modified oil palm boiler ash (OPBA) biosorbent. J Clean Prod, 230: 527-535, doi: 10.1016/j.jclepro.2019.04.390.

[18] J. Magiera and R. Katulski. 2015. Journal of applied research and technology. Journal of Applied Research and Technology, 13(1): 45-57, [Online]. Available: https://www.redalyc.org/articulo.oa?id=47436895004

[19] J. Zhang, Z. Guo, X. Zhi and H. Tang. 2013. Surface modification of ultrafine precipitated silica with 3-methacryloxypropyltrimethoxysilane in carbonization process. Colloids Surf a Physicochem Eng Asp, 418: 174-179, doi: 10.1016/j.colsurfa.2012.11.057.

[20] L. T. Zhuravlev. 2000. The surface chemistry of amorphous silica. Zhuravlev model. Colloids Surf a Physicochem Eng Asp, 173(1-3): 1-38, doi: 10.1016/S0927-7757(00)00556-2.

[21] A. Egerton. 1957. Encyclopædia of chemical technology. Nature, 179(4568): 983-984, doi: 10.1038/179983a0.

[22] H. Ismail and F. S. Haw. 2010. Curing characteristics and mechanical properties of hybrid palm ash/silica/natural rubber composites. Journal of Reinforced Plastics and Composites, 29(1): 105-111, doi: 10.1177/0731684408096423.

[23] S. O. Bamaga, M. W. Hussin and M. A. Ismail. 2013. Palm Oil Fuel Ash: Promising supplementary cementing materials. KSCE Journal of Civil Engineering, 17(7), doi: 10.1007/s12205-013-1241-9.

[24] S. Thongsang, W. Vorakhan, E. Wimolmala and N. Sombatsompop. 2012. Dynamic mechanical analysis and tribological properties of NR vulcanizates with fly ash/precipitated silica hybrid filler. Tribol Int, 53: 134-141, doi: 10.1016/j.triboint.2012.04.006.

[25] M. N. A. Uda *et al*. 2021. Production and characterization of silica nanoparticles from fly ash: conversion of agro-waste into resource. Prep Biochem Biotechnol, 51(1): 86-95, doi: 10.1080/10826068.2020.1793174.

[26] S. G. D. Iya, M. Z. Noh, S. N. Ab Razak and N. A. A. Kutty. 2017. Physical and Mechanical Properties of Porcelain Formed by Substituting Quartz with HCl Treated Palm Oil Fuel Ash. Journal of Science and Technology. 9(3): 160-164.

[27] O. V. Gorbunova, O. N. Baklanova, T. I. Gulyaeva, M. V. Trenikhin and V. A. Drozdov. 2014. Poly (ethylene glycol) as structure directing agent in sol-gel synthesis of amorphous silica. Microporous and Mesoporous Materials, 190: 146-151, doi: 10.1016/j.micromeso.2014.02.013.

[28] J. Li, X. Hu, C. Zhang, W. Luo and X. Jiang. 2021. Enhanced thermal performance of phase-change materials supported by mesoporous silica modified with polydopamine/nano-metal particles for thermal energy storage. Renew Energy, 178: 118-127, doi: 10.1016/j.renene.2021.06.021.

[29] E. M. Ginting, N. Bukit, Motlan, M. T. Saragih, E. Frida and B. F. Bukit. 2020. Analysis of natural rubber compounds with filler of Oil Palm Empty Bunches Powder and Carbon Black. J Phys Conf Ser, 1428(1), doi: 10.1088/1742-6596/1428/1/012024.

[30] N. Bukit, E. M. Ginting, E. A. Hutagalung, E. Sidebang, E. Frida and B. F. Bukit. 2019. Preparation and characterization of oil palm ash from boiler to nanoparticle. Reviews on Advanced Materials Science, 58(1): 195-200, doi: 10.1515/rams-2019-0023.

[31] V. S. Abhisha, A. Augustine, J. Joseph, S. P. Thomas and R. Stephen. 2020. Effect of halloysite nanotubes and organically modified bentonite clay hybrid filler system on the properties of natural rubber. Journal of Elastomers and Plastics, 52(5): 432-452, doi: 10.1177/0095244319865573.

[32] V. Tambrallimath *et al*. 2022. Synthesis and characterization of flyash reinforced polymer composites developed by Fused Filament Fabrication. Journal of Materials Research and Technology, 21: 810-826, doi: 10.1016/j.jmrt.2022.09.059.